Towards A Single Electron Current On Superfluid Helium

Oliver Funk
Department of Electrical Engineering
University Of Cape Town
Cape Town, South Africa
oli.funk@gmail.com

Dr Mark Blumenthal
Department of Physics
University Of Cape Town
Cape Town, South Africa
mark.blumenthal@uct.ac.za

Dr Fred Nicolls
Department of Electrical Engineering
University Of Cape Town
Cape Town, South Africa
fred.nicolls@uct.ac.za

***Abstract*—The aim of this thesis was to investigate the application of a system of electrons floating above the surface of superfluid helium to the field of single electron transport. Previous work done by Dr Forrest Bradbury at Princeton University (now a collaborator of our group) demonstrated the highly efficient and precise control of packets of electrons floating on the surface of superfluid helium, localised to channels defined in a silicon substrate.**

Using similar devices and methodologies, we are investigating whether this modality of electron transport can be effectively applied to deliver a current of single electrons.

Presented in this paper is a summary of the work completed to date in my thesis, namely: the fabrication of the nanostructure semiconductor substrate at Oak Ridge National Labs in the USA, the electronics for the data acquisition system, the hermetically sealed superfluid cell designed in collaboration with Dr Jay Amrit from Université Paris-Sud, France, as well the probe needed to insert the cell into the dilution fridge.

I. Introduction

Electrons on superfluid helium present an opportunity to investigate a physical system with unique and interesting properties. Electrons will become bound to the surface of the superfluid by their own image potential induced in the weakly polarizable fluid, which attracts them towards it. However, they are prevented from breaking through it due to the large energy barrier ($\sim 1\,\mathrm{eV}$) established by the Pauli exclusion principle [1]. These opposing energies create a potential environment in which the charges will, in their ground state, float approximately $100\,\text{Å}$ above the surface, forming a two-dimensional electron gas system (2DEG) above the surface.

A 2DEG established in this manner has a very low density and is thus in a purely non-degenerate state. This is mainly caused by the strong Coulomb interactions between the charges which are largely unscreened given the very small dielectric constant of liquid helium ($\epsilon_r \simeq 1.057$). The charges in this system are also very well isolated above the fluid film and exhibit some of the highest mobilities of any system (exceeding $10^7 \mathrm{cm/Vs}$ [2]), due to the minimal scattering events that can occur given the properties of superfluid $^4\mathrm{He}$. These two distinguishing characteristics have been used to study a wide variety of different physical phenomena such as investigating the topological surface structure of superfluid $^4\mathrm{He}$ [3], Wigner crystallisation [4], Coulomb liquids [5]) and as a way to implement a scalable quantum computing chip [6].

The high mobilities of the charges in this system could be applied to the field of Single Electron Transport (SET) to deliver an accurate single electron current that can remain coherent for a long period of time. This is the main reason for the focus of this thesis on this work. The novel application of this type of charge system to the field of SET could allow one to explore SET in a competently new regime, where experiments that require single electrons with high mobilities and coherence times can be performed.

This work was inspired by the previous work done by Bradbury et al. [7] at Princeton University, who demonstrated precise and efficient control over the position of packets of charges along superfluid $^4\mathrm{He}$ channels. The work by Papageorgiou et al. [8] demonstrated the ability to count individual electrons passing in and out of a quantum dot above superfluid films, and by Rees et al. [9] and Lin et al. [10], who implemented split gates in superfluid $^4\mathrm{He}$, also gave merit to the application of the system to SET.

In summary, the following research questions were asked to focus the scope and drive of this thesis:

- Can a controllable single electron current be achieved using the modality of electrons on superfluid $^4\mathrm{He}$?
  More precisely, after pumping electrons at a certain frequency for a period of time, does the total theoretical amount of transported charge Q_{theo} correspond to the amount measured using the capacitive charge sensing technique Q_{meas}?
- Can this accumulated charge be drained as a direct current? If so, does the total current measurement correspond to the amount sensed (Q_{meas} from the above)?

II. Literature

A. Single Electron Devices

Single electron devices fall into the SET field of study and have numerous applications in the field of quantum metrology and quantum information processing [11]. These devices produce a single electron current defined by the characteristic equation

$$I_{SET} = ne f_{SET}\,, \tag{1}$$

where

n is the number of electrons transported per cycle,
e is the universal elementary charge of the electron,
f_{SET} is the transport frequency.

An area of active research is in trying to get magnitude and measurement uncertainty of the single electron current to a point where it can replace the existing SI definition of the ampere, which uses a link between a current-induced force to a kilogram. This is part of an on-going effort in trying to redefine SI base units in terms of universal physical constants. For example, the volt is now defined using the Josephson effect realised on a superconducting Josephson junction and the Ohm using the quantum Hall effect [12]. Electrical current can be derived using these two standards via Ohm's law, however, a direct independent measurement would allow for greater precision in the value and validate the other two measurements. This would close the so-called quantum metrological triangle (QMT) [12].

To achieve this, an uncertainty of less than 10^{-7} must be achieved in the measured single electron current, at magnitudes in the microampere range in order to be practically useful [11].

Some of the first single electron devices were developed around the 1990s [13], [14], [15], based on the single electron transistor initially developed at Bell labs [16]. These were called *single electron turnstile* devices as they had two-door gates on either side of a tunable quantum dot capacitively coupled to a 'turnstile' gate, which could control the energy levels of the dot to let a single electron through per cycle.

Enough of a separation between the dot's energy levels could be achieved as the devices were fabricated using the then-new silicon-based GaAs/AlGaAs heterostructures. This allowed for very small quantum dots to be made, reducing the dot's self-capacitance C_Σ (the capacitance between the dot and its surroundings), making the charging energy of the dot $E_c = \mathrm{e}^2/C_\Sigma$ (the difference between energy levels) acceptably large.

These devices, however, relied on the stochastic process of electron tunnelling which limited their operational frequency, meaning the output current was very small. Geerlings et al. [13] showed that the tunnelling rate Γ proportional to $(RC)^{-1}$, with the expected probability for an electron to miss a cycle being $p_m \simeq \exp(-\Gamma/f)$. Therefore the transport frequency f had to be kept low, as $f \ll (RC)^{-1}$ was required to realise a current of acceptable accuracy.

Later, the so-called *single electron pumps* were developed which used the potential profiles established by various gates to create a quantum dot cable of holding a single (or possibly more) electron. Once captured, the electron could be ejected by raising its potential above an exit gate barrier [17], [18], [19].

Progress on the pumps was made and saw the development of the first quantised acoustoelectric transport using surface acoustic (SAW) waves [20], [21], [22] improving the accuracy and frequency into the GHz range. Further developments the field of nano-fabrication led Blumenthal et al. [23] to develop the first gigahertz electron pump, allowing for a current output in the order of hundreds of picoamps to be measured at an accuracy of 10^{-4}.

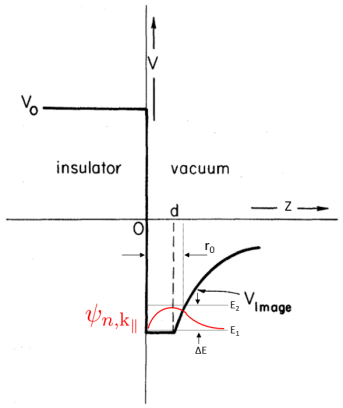

Fig. 1. Electron wave-function (in red) inside the self-induced image potential in the liquid's surface, adapted from Cole and Cohen [25].

More recent studies have shown that a 150 pA current can be attained at a standard uncertainty of 6.5×10^{-7}, after 15 hours of averaging [24], [11].

One of the possible advantages of using a superfluid helium system for SET is the ability to scale the number of electrons being transported per cycle (i.e. n from Eq. (1)). Using a device with multiple channels, one can transport multiple electrons in parallel as very good uniformity can be achieved between channels (unlike in heterostructures), while maintaining acceptable levels of accuracy by keeping the transport frequency f_{SET} low.

B. Electrons On Superfluid Helium

a) Background: The system of electron on superfluid helium as first investigated by Sommer in 1964 [1], showing that liquid ^{4}He will appear as an energy barrier of $\sim 1\,\mathrm{eV}$ to electrons and that they form a self-induced image potential cavity on the liquid's surface. Cole and Cohen [25], [26] followed by examining the properties of image potentials induced in the surface of insulators at low temperatures.

An important result from Sommer and Tanner [27] showed a method for measuring the mobility of the charges using electrodes placed just underneath the top of the liquid's surface. The resulting phase shift of a signal applied to an electrode, capacitively coupled through the surface charges, could be measured and related to the charge system's mobility.

Later, interest in the applicability of the system to quantum computing became evident after studies proposed using the high mobilities of the charge system to maintain coherence for long periods of time [28], [29], [6], [30].

Papageorgiou et. al. [8] in 2005 used a superconducting single-electron transistor as an electrometer placed underneath the helium film to count the number of electrons trapped inside the pool above. They observed the distinctive Coulomb staircase as electrons left the dot one by one. In 2011 Bradbury et. al. [7] demonstrated precise and efficient control over the

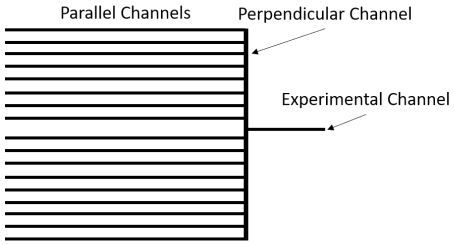

Fig. 2. A simplified diagram of the central part of the device, showing the three main channel regions.

positions of electrons in channels, being able to move them by strong coupling to gate electrodes underneath the surface of the fluid, thus allowing efficient clocking of the electrons in a CCD type fashion. Rees et al. [9] and Lin et al. [10] instigated the transport characteristics of the system using split gates to trap individual charges.

b) Theory: The self-induced image potential

$$V_{\text{image}}(z) = -\frac{\Lambda \mathrm{e}^2}{z}\,,\ \Lambda = \frac{1}{4}\cdot\frac{\epsilon_{\text{He}}-1}{\epsilon_{\text{He}}+1}\,, \tag{2}$$

in the liquid's surface quantises the electron's vertical motion and traps the charge above it, as shown in Fig. 1.

Because there are no confining potentials in the x, y-plane parallel to surface, the following Schrödinger equation:

$$\left[-\frac{\hbar^2}{2\mathrm{m}_{\parallel}}\nabla^2_{x,y} - \frac{\hbar^2}{2\mathrm{m}_{\perp}}\frac{\partial^2}{\partial z^2} + V_{\perp}(z)\right]\psi = E\psi\,, \tag{3}$$

can be used to model the system.

It can be shown that the allowed quantised vertical energies are given by

$$E_n = -\frac{m_{\perp}\mathrm{e}^4}{2\hbar^2}\left[\frac{\Lambda}{n}\right]^2 = -\mathrm{R}\left[\frac{\Lambda}{n}\right]^2\,, \tag{4}$$

where $m_{\perp}$ is taken to be the free-electron mass $\mathrm{m_e}$ and R = 13.6 eV is the Rydberg energy.

The ground-state energy is thus $E_1 \simeq -0.7\,\text{meV} \to 8.1\,\text{K}$ and the first excited state is $E_2 \simeq -0.16\,\text{meV} \to 1.9\,\text{K}$. The expectation value of the perpendicular distance for the ground-state from the fluid's surface is approximately given by an effective Bohr radius of $\langle z\rangle_{\varphi_0} = r_0 = \hbar^2/\mathrm{m_e e^2}\Lambda \simeq 100\,\text{Å}$. These results also show that a 2DEG does indeed form above the surface of the superfluid.

c) Charge Detection: The method originally proposed by Sommer and Tanner [27] can be adapted to measure the number of electrons (quantity of charge) above two gates, a twiddle and a sense gate, by oscillating the charges back and forth at a known frequency and measuring the difference in the magnitude of the sensed signal compared to the original signal. This difference can be related to the total number of electrons present. This method can be applied to SET, giving a way to measure the total amount of pumped charge.

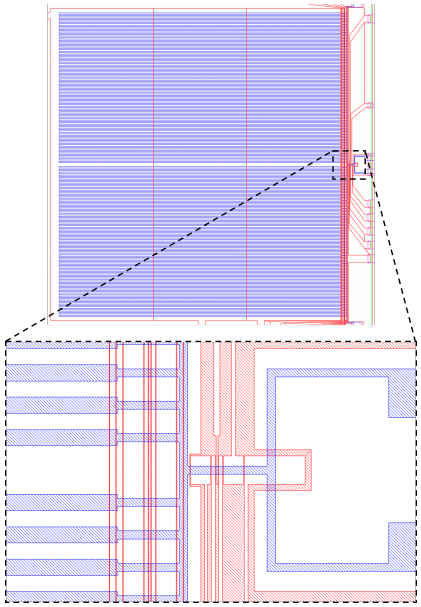

Fig. 3. The CAD model for the central part of the device, with a close up of the experimental channel. The channels are in purple and the bottom gates are in red.

III. Device Design And Fabrication

A. Overview

The device consisted of two main sections: a 'parallel channels' section with 120 channels and an 'experimental channel' section with only one channel, which were connected together by another 'perpendicular channel'. Fig. 2 shows a simplified diagram of this layout. Fig. 3 shows a close-up of the central part of the CAD model used to define the device geometry.

Both sections of the device had turnstile gates (for the single electron transport) and charge detection gates implemented in them. The idea was that if quantised transport could not be achieved in the parallel channels, maybe it could be in the single experimental channel. Both sections also had top gates to be used to drain the transported charge away as conventional current.

The device would be charged by electrons thermally emitted from a tungsten filament placed above the device. Three large gates (seen in the top image in Fig. 3) underneath the parallel channels section would be set to a positive potential to attract the electrons to the device, filling the channels.

B. Modelling

a) Charge Sensing: Two gates, a twiddle V_{tw} and a sense V_s gate, were implemented into the device to measure the amount of charge in the region above them. By applying a sinusoidal driving signal at frequency f_{tw} to the twiddle gate, which is capacitively coupled through the charge system to the sense gate, one can measure the difference in the magnitude of the sensed signal ΔV (compared to when there are no charges) which can be related back to the amount of charge present.

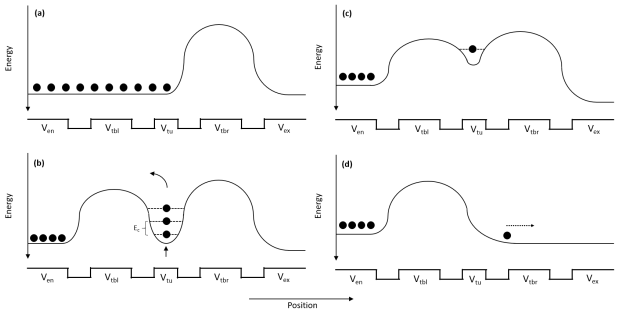

Fig. 4. Potential profile at the fluid surface above the turnstile gates during one cycle.

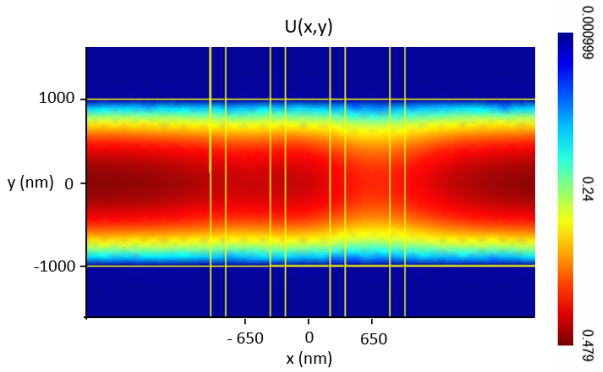

Fig. 5. An finite element model of potential at the surface $U(x, y)$ around the turnstile gates, at a moment in time during a pumping cycle.

This difference is expressed as

$$\Delta V = |V_{s,a}(f)|_{f=f_{tw}} - |V_{s,b}(f)|_{f=f_{tw}} \tag{5}$$

where $V_{s,b}$ is the sensed signal *before* any charges are present in the sensing region (i.e. the baseline measurement) and $V_{s,a}$ is the signal *after* ΔQ_e of charge is present the sensing region. The magnitude of the sensed signal at the twiddle frequency is the final output from the lock-in amplifier, which is why the magnitude are used in Eq. (5).

It can shown that, if a high enough twiddle frequency f_{tw} and output resistance R_o is used (which are design parameters that can easily be controlled)

$$\Delta V \simeq \frac{\Delta Q_e}{C_\Sigma} \,. \tag{6}$$

Additionally, if we assume the input capacitance of the High Electron Mobility Transistor (HEMT) C_{gs} dominates over the other capacitances such $C_\Sigma \simeq C_{gs} \simeq 1\,\mathrm{pF}$ and one electron is present in all 120 channels, the expected increase in the magnitude of the sensed signal will be

$$\Delta V = 120 \cdot \frac{1.6 \times 10^{-19}\,\mathrm{C}}{1\,\mathrm{pF}} = 19.2\,\mu\mathrm{V} \,. \tag{7}$$

b) Single Electron Turnstile: A system of gates were used to implement the single electron turnstile. A central 'turnstile' gate V_{tu} was used with two barrier gates on the left V_{tbl} and right V_{tbr} of it. An entrance and exit gate (V_{en} and V_{ex}) were used, which determined the entrance and exit potentials of the charges and acted as reservoirs for the charges before and after being pumped.

One of the main benefits of using superfluid helium as the substrate for a single electron device is the lack of screening caused by the helium film, making the Coulomb potential U_{co} between charges strong. It will thus contribute significantly to the charging energy E_c of the quantum dot above the turnstile gate:

$$E_c = \mathrm{e}^2/C_\Sigma + U_{co} \,, \tag{8}$$

$$U_{co} = \frac{\mathrm{e}^2}{4\pi\epsilon_{\mathrm{He}}} \frac{1}{r_c} \,, \tag{9}$$

where r_c is the distance between the charges.

In the case of the device that was fabricated, $r_c = w_{tu} \simeq 0.5\,\mu\mathrm{m}$ making $U_{co} \simeq 2.7\,\mathrm{meV}$.

In order to achieve deterministic single electron transport, a single charge must become trapped in the potential well created above the turnstile gate during each transport cycle. The depth of this well ΔU_w would thus need be greater than the thermal energy of an electron, which at $T = 1\,\mathrm{K}$ $E_{th} = \mathrm{k_B}T \simeq 0.09\,\mathrm{meV}$, but less than the dot's charging E_c. If it is assumed that the charging energy was dominated by the Coulomb potential, then $E_c \simeq U_{co} \simeq 2.7\,\mathrm{meV}$. If $\Delta U_w > E_c$ then more than one charge could be present inside the dot at one time.

After conducting multiple FEM simulations of the device, a sample is shown in Fig. 5, it was found the following gates voltages: $V_{en} = V_{ex} = 1\,\mathrm{V}, V_{tbl} = 0.95\,\mathrm{V}, V_{tbr} = 0.9\,\mathrm{V}, V_{tu} = 1.05\,\mathrm{V}$ produced a well depth of $\Delta U_w = 1.3\,\mathrm{meV}$ at the surface, which would successfully isolate a single electron.

Fig. 4 shows the sequence of steps involved in clocking a single charge through the turnstile gates.

C. Fabrication

The device consisted of three layers: the bottom gates, the middle channel walls and the top metal. There were six lithography layers involved in the device's fabrication.

The first layers two defined the bottom gates using an initial deposition of a metal stack of $5\,\mathrm{nm}$ Chromium (Cr), $20\,\mathrm{nm}$ Gold (Au), $3\,\mathrm{nm}$ Cr. The thin Cr layers were needed as adhesive layers between the Au layer and the various oxides surrounding it. This was followed by an etch defined using Electron Beam Lithography (EBL). EBL was needed to define the narrow $150\,\mathrm{nm}$ gap sizes between the gates. The third layer defined the bond pads and the traces that connected the bond pads to the bottom gates.

This was followed by a deposition of various oxides needed to define the middle layer of the device for the channel walls. A combination of Plasma-Enhanced Chemical Vapour Deposition (PECVD) and Atomic Layer Deposition (ALD) techniques were employed.

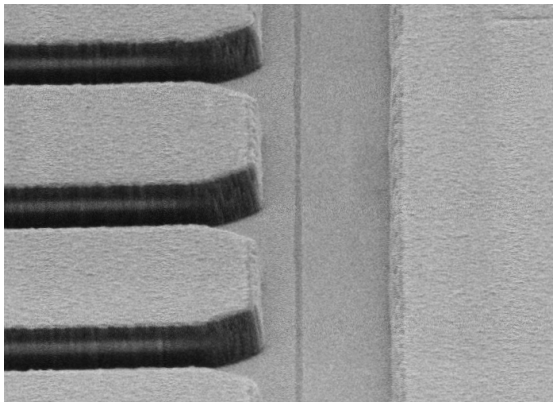

Fig. 6. An angled SEM image of the ends of the 2 µm wide micro-channels in a device.

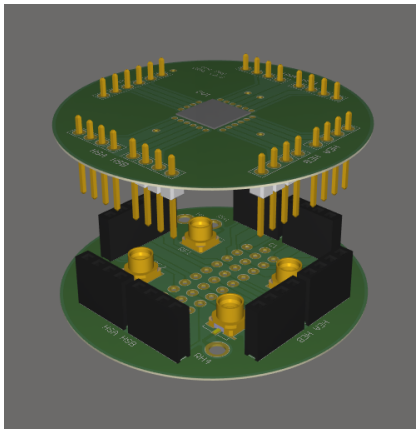

Fig. 7. A render of the two primary PCBs and how they connect to each other. On top is the Device Holding Board, that the fabricated device is connected to, and on the bottom is the Motherboard, that interfaces with the connectors present inside the cell.

The fourth and fifth layers defined simple squares and thickening areas depositions for the top metal.

Finally, the sixth layer defined an etch mask for the channel geometry. It was the most complicated step in the whole fabrication process, involving an initial sputter etch through the top metal, followed by a Reactive Ion Etching (RIE) through the middle of the device to define the channel walls and finally a BHF 50:1 wet chemistry etch to remove the last bits of oxide left. This layer was complicated due to the fine geometry of the channels but also because of the required alignment tolerances, the need to keep the channel walls smooth and the need to not roughen the bottom gates when etching.

Fig. 6 shows the ends of some of the micro-channels channels fabricated into the device. One can the darker parts, which are the channel walls and the lighter parts are the metals for the top and bottom gates.

IV. Electronics

Electronics defined on Printed Circuit Boards (PCBs) were needed to control and read signals from the device's gates, to which it is connected. Two primary PCBs were created for this project, one stacked on top of another (as shown in Fig. 7).

The bottom board, called the Motherboard (MBD), interfaced with the connectors present in the cell (a 31-pin connector for bias voltages and another four co-axial pins for sensitive, oscillatory signals). Connecting into it from above was the Device Holding Board (DHB), that was wire bonded to the fabricated device. Two HEMT pre-amplifiers were built into the DHB to amplify the very weak signals from the sense gate used during charge measurements.

These boards were designed using Altium and fabricated in Cape Town by Trax. (Pty.) Ltd.

V. Cell & Dilution Fridge Probe

The hermetically sealed superfluid cell shown in Fig. 8 was designed in collaboration with Dr Jay Amrit from Université Paris-Sud, France. The bottom of the cell has four feed-through connectors for the RF lines and a central 31-pin connector for the bias voltages. The top of the cell has a superfluid helium fill line coming in from the top as well as a circular connector that provides the additional pins needed for the tungsten filament for the thermal emission of electrons, as well as for miscellaneous components such as a depth measurement device to measure the bulk superfluid level.

The cell was made superfluid leak-tight using Kapton seals with an interlocking connection between the vacuum chamber and the cell flange.

An important aspect that needed to be taken into consideration was good thermal anchoring of the cell to the probe that lowered it into the bottom of the dilution fridge. If the contact surface area was not sufficiently large, it would take extremely long to cool the cell down.

VI. Conclusion

The work done in this thesis has laid down the foundation needed to take this project further. The various lock-downs instituted globally due to the COVID-19 pandemic severely limited the scope of this thesis. A working device could not be fabricated in time, therefore no concrete result to the research questions stated in the introduction can be presented.

The main contributions of this thesis have been the device design, modelling and fabrication process that was developed at ORNL. The design and fabrication of the PCBs needed for the data acquisition system have also been important contributions.

Additionally, the relationship that has been developed with Oak Ridge National Labs during this thesis has also been very important. It will give future interested students from the NanoElectronics group the opportunity to get hands-on experience with nano-fabrication and the advanced equipment they have in the cleanroom there.

Future students working on this project should be able to get the first experimental results of electron on superfluid helium on the African continent, which I believe is something worth pursuing.

Further work is needed to finalise the fabrication of the device and have one successfully made. Integrating it with

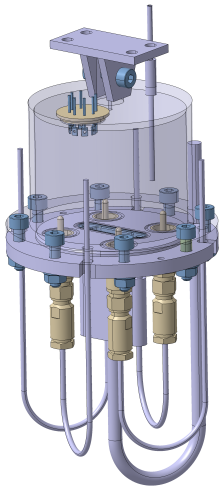

Fig. 8. A render of the hermetic cell assembly. Image from Dr Jay Amrit, Université Paris-Sud. The PCBs shown in Fig. 7 fit inside of the main vacuum chamber and connect to the various connectors present.

the electronics inside the fridge and getting initial readings would then need to take place. Finding suitable potentials waveforms to apply to the turnstile gates to achieve quantised single electron transport would need to be done as well as successfully performing charge detection measurements.

Acknowledgment

I would like to thank my supervisors Prof. Mark Blumenthal and Prof. Fred Nicolls for their support, guidance, and feedback throughout this masters project. Dr Forrest Bradbury for the contributions he made to the design of the device and areas of the modelling. Jacob Swett and the team at Oak Ridge National Labs for their support and guidance during the device fabrication stages.

References

[1] W. T. Sommer, "Liquid helium as a barrier to electrons," *Phys. Rev. Lett.*, vol. 12, pp. 271–273, Mar 1964.

[2] K. Shirahama, S. Ito, H. Suto, and K. Kono, "Surface study of liquid helium-3 using surface state electrons," *Journal of Low Temperature Physics*, vol. 101, pp. 439–444, Nov 1995.

[3] K. Kono, "Electrons on the surface of superfluid helium 3," *Journal of Low Temperature Physics*, vol. 158, no. 1-2, p. 288, 2010.

[4] C. C. Grimes and G. Adams, "Evidence for a liquid-to-crystal phase transition in a classical, two-dimensional sheet of electrons," *Phys. Rev. Lett.*, vol. 42, pp. 795–798, Mar 1979.

[5] Y. Monarkha and K. Kono, *Two-dimensional Coulomb liquids and solids*, vol. 142. Springer Science & Business Media, 2013.

[6] S. A. Lyon, "Spin-based quantum computing using electrons on liquid helium," *Phys. Rev. A*, vol. 74, p. 052338, Nov 2006.

[7] F. R. Bradbury, M. Takita, T. M. Gurrieri, K. J. Wilkel, K. Eng, M. S. Carroll, and S. A. Lyon, "Efficient clocked electron transfer on superfluid helium," *Phys. Rev. Lett.*, vol. 107, p. 266803, Dec 2011.

[8] G. Papageorgiou, P. Glasson, K. Harrabi, V. Antonov, E. Collin, P. Fozooni, P. G. Frayne, M. J. Lea, D. G. Rees, and Y. Mukharsky, "Counting individual trapped electrons on liquid helium," *Applied Physics Letters*, vol. 86, no. 15, p. 153106, 2005.

[9] D. G. Rees, I. Kuroda, C. A. Marrache-Kikuchi, M. Höfer, P. Leiderer, and K. Kono, "Transport measurements of strongly correlated electrons on helium in a classical point-contact device," *Journal of Low Temperature Physics*, vol. 166, pp. 107–124, Feb 2012.

[10] J.-Y. Lin, A. V. Smorodin, A. O. Badrutdinov, and D. Konstantinov, "Transport properties of a quasi-1d wigner solid on liquid helium confined in a microchannel with periodic potential," *Journal of Low Temperature Physics*, vol. 195, pp. 289–299, May 2019.

[11] B. Kaestner and V. Kashcheyevs, "Non-adiabatic quantized charge pumping with tunable-barrier quantum dots: a review of current progress," *Reports on Progress in Physics*, vol. 78, no. 10, p. 103901, 2015.

[12] M. W. Keller, "Current status of the quantum metrology triangle," *Metrologia*, vol. 45, no. 1, p. 102, 2008.

[13] L. J. Geerligs, V. F. Anderegg, P. A. M. Holweg, J. E. Mooij, H. Pothier, D. Esteve, C. Urbina, and M. H. Devoret, "Frequency-locked turnstile device for single electrons," *Phys. Rev. Lett.*, vol. 64, pp. 2691–2694, May 1990.

[14] L. P. Kouwenhoven, A. T. Johnson, N. C. van der Vaart, C. J. P. M. Harmans, and C. T. Foxon, "Quantized current in a quantum-dot turnstile using oscillating tunnel barriers," *Phys. Rev. Lett.*, vol. 67, pp. 1626–1629, Sep 1991.

[15] Y. Nagamune, H. Sakaki, L. Kouwenhoven, L. Mur, C. Harmans, J. Motohisa, and H. Noge, "Single electron transport and current quantization in a novel quantum dot structure," *Applied physics letters*, vol. 64, no. 18, pp. 2379–2381, 1994.

[16] T. A. Fulton and G. J. Dolan, "Observation of single-electron charging effects in small tunnel junctions," *Phys. Rev. Lett.*, vol. 59, pp. 109–112, Jul 1987.

[17] H. Pothier, P. Lafarge, C. Urbina, D. Esteve, and M. H. Devoret, "Single-electron pump based on charging effects," *Europhysics Letters (EPL)*, vol. 17, pp. 249–254, jan 1992.

[18] M. W. Keller, J. M. Martinis, N. M. Zimmerman, and A. H. Steinbach, "Accuracy of electron counting using a 7-junction electron pump," *Applied Physics Letters*, vol. 69, no. 12, pp. 1804–1806, 1996.

[19] M. H. Devoret, D. Esteve, and C. Urbina, "Single-electron transfer in metallic nanostructures," *Nature*, vol. 360, no. 6404, pp. 547–553, 1992.

[20] V. I. Talyanskii, J. M. Shilton, M. Pepper, C. G. Smith, C. J. B. Ford, E. H. Linfield, D. A. Ritchie, and G. A. C. Jones, "Single-electron transport in a one-dimensional channel by high-frequency surface acoustic waves," *Phys. Rev. B*, vol. 56, pp. 15180–15184, Dec 1997.

[21] N. E. Fletcher, J. Ebbecke, T. J. B. M. Janssen, F. J. Ahlers, M. Pepper, H. E. Beere, and D. A. Ritchie, "Quantized acoustoelectric current transport through a static quantum dot using a surface acoustic wave," *Phys. Rev. B*, vol. 68, p. 245310, Dec 2003.

[22] J. Ebbecke, N. E. Fletcher, T. J. B. M. Janssen, H. E. Beere, D. A. Ritchie, and M. Pepper, "Acoustoelectric current transport through a double quantum dot," *Phys. Rev. B*, vol. 72, p. 121311, Sep 2005.

[23] M. D. Blumenthal, B. Kaestner, L. Li, S. Giblin, T. J. B. M. Janssen, M. Pepper, D. Anderson, G. Jones, and D. A. Ritchie, "Gigahertz quantized charge pumping," *Nature Physics*, vol. 3, pp. 343–347, May 2007.

[24] M. Wulf, "Error accounting algorithm for electron counting experiments," *Phys. Rev. B*, vol. 87, p. 035312, Jan 2013.

[25] M. W. Cole and M. H. Cohen, "Image-potential-induced surface bands in insulators," *Phys. Rev. Lett.*, vol. 23, pp. 1238–1241, Nov 1969.

[26] M. W. Cole, "Properties of image-potential-induced surface states of insulators," *Phys. Rev. B*, vol. 2, pp. 4239–4252, Nov 1970.

[27] W. T. Sommer and D. J. Tanner, "Mobility of electrons on the surface of liquid ^{4}He," *Phys. Rev. Lett.*, vol. 27, pp. 1345–1349, Nov 1971.

[28] P. Platzman and M. Dykman, "Quantum computing with electrons floating on liquid helium," *Science*, vol. 284, no. 5422, pp. 1967–1969, 1999.

[29] M. Dykman, P. Platzman, and P. Seddighrad, "Qubits with electrons on liquid helium," *Physical Review B*, vol. 67, no. 15, p. 155402, 2003.

[30] G. Koolstra, G. Yang, and D. I. Schuster, "Coupling a single electron on superfluid helium to a superconducting resonator," *Nature communications*, vol. 10, no. 1, pp. 1–7, 2019.